Global Biogeochemical Cycles

RESEARCH ARTICLE
10.1029/2026GB009099

An Optimal Approach for Assessment of Dust Fluxes to the Ocean Using ^{232}Th and ^{230}Th

George H. Rowland[1,2] and **Gideon M. Henderson**[1]

[1]Department of Earth Sciences, University of Oxford, Oxford, UK, [2]Now at Institute for Marine and Antarctic Studies, University of Tasmania, Hobart, TAS, Australia

Key Points:

- Apparent dust fluxes to the ocean calculated using ^{232}Th/^{230}Th increase strongly with water depth
- Model thorium profiles indicate that existing methods overestimate dust fluxes at the greatest water depths by ~2 times
- An alternative method for estimating ^{230}Th residence time allows more accurate dust fluxes to be calculated from ^{232}Th/^{230}Th measurements

Supporting Information:

Supporting Information may be found in the online version of this article.

Correspondence to:

G. H. Rowland,
george.rowland@utas.edu.au

Citation:

Rowland, G. H., & Henderson, G. M. (2026). An optimal approach for assessment of dust fluxes to the ocean using ^{232}Th and ^{230}Th. *Global Biogeochemical Cycles*, *40*, e2026GB009099. https://doi.org/10.1029/2026GB009099

Received 25 JAN 2026
Accepted 28 APR 2026

Author Contributions:

Conceptualization: George H. Rowland, Gideon M. Henderson
Formal analysis: George H. Rowland, Gideon M. Henderson
Funding acquisition: Gideon M. Henderson
Investigation: George H. Rowland, Gideon M. Henderson
Methodology: George H. Rowland
Project administration: Gideon M. Henderson
Resources: Gideon M. Henderson
Supervision: Gideon M. Henderson
Visualization: George H. Rowland, Gideon M. Henderson
Writing – original draft: George H. Rowland

Abstract Quantifying fluxes of mineral dust to the ocean surface is important for understanding ocean biogeochemical cycles and climate. Geochemical methods can provide dust flux estimates, including through the application of ^{232}Th/^{230}Th. This use of thorium isotopes has been hindered, however, by the ubiquitous presence of strong vertical increases in calculated ^{232}Th (and therefore dust) fluxes with water depth. Such increases cannot realistically reflect changing dust fluxes with depth, so demonstrate a limitation in the thorium isotope approach. To investigate the origins of apparent increases in flux with depth, we have applied a one-dimensional reversible scavenging model to produce idealized profiles of ^{230}Th and ^{232}Th, and have used that model to test existing approaches to flux assessment and to develop an improved method. Our model and field data indicate that ^{232}Th is released from dust over the upper few hundred meters of the water column. In this depth range, traditional use of integrated ^{230}Th residence times (τ_{230}) to calculate ^{232}Th fluxes may be reasonable because the source terms of both isotopes are similar and approximately constant with depth. At greater water depths, integrated τ_{230} overestimates the ^{232}Th flux by a factor that approaches 2, due to the different depth distributions of ^{232}Th and ^{230}Th addition. We suggest a new approach to calculate τ_{230}, which relies on in situ concentrations of ^{230}Th at each depth, rather than an integrated value. Using this "volumetric" approach yields ^{232}Th fluxes that are broadly constant with depth and which more accurately capture the true ^{232}Th flux.

Plain Language Summary Calculating how much desert dust lands on the ocean is important because the dust provides nutrients to tiny marine plants which controls their growth. Directly measuring dust falling on the ocean is difficult as the ocean is so large and mostly remote. One method to calculate dust input rates uses measurements of two types of the element thorium. A problem with this method is that the dust deposition rate appears to increase when measured at greater water depths—something that does not fit with dust landing on the ocean surface. We used equations and a known dust input to predict thorium concentrations at different ocean depths. We then used our predictions to back-calculate the dust input using the existing calculation method. We found that the method calculates the correct amount of dust near the surface ocean, but at greater depths it produces dust deposition rates that are almost two times too large. This happens because the two types of thorium follow different pathways, and so do not spend the same amount of time in the ocean. We developed a new version of the method that removes the increases with depth and gives a better estimate of dust deposition.

1. Introduction

Mineral dust is an important climatic variable that influences the radiation budget of Earth and delivers nutrients to remote ocean ecosystems (Maher et al., 2010). Particular interest in dust fluxes to the surface ocean has been stimulated by the links between the micronutrient iron, phytoplankton and cycling of CO_2, particularly in high-nutrient low-chlorophyll regions (Buchanan et al., 2019; Hamilton et al., 2020; Jickells & Moore, 2015; Martin, 1990; Martínez-García et al., 2014; Weis et al., 2024). Dust fluxes to the ocean remain uncertain in the modern day despite studies using aerosol collection, sediment traps, dust deposition modeling, satellite observations and ocean geochemistry (Anderson et al., 2016; van der Does et al., 2020; Wu et al., 2020; Yu et al., 2019). Agreement between different methods is often limited to within a factor of 10 or more and observations are sparse or missing over much of the ocean (Wu et al., 2020).

One method for estimating dust fluxes uses measurements of dissolved lithogenic elements or isotopes that have short residence times in seawater (e.g., Al and ^{232}Th). The conceptual model assumes that the supply of these

Writing – review & editing: George H. Rowland, Gideon M. Henderson

species to the ocean is solely from the dissolution of dust near the surface, and that there is a steady-state between inputs and outputs (Anderson et al., 2016; Hsieh et al., 2011; Measures & Vink, 2000). Combining the inventory of a lithogenic tracer (X, μg m^{-2}) in seawater with its residence time (τ, years) over a depth-interval (0–z, m) provides an estimate of its steady-state flux (F_X, μg m^{-2} yr^{-1}) to the surface:

$$F_X\left[\mu g\ m^{-2}\ yr^{-1}\right] = \frac{\int_0^z X dz}{\tau}\left[\frac{\mu g\ m^{-2}}{yr}\right] \quad (1)$$

To calculate a dust flux from the resulting flux of the lithogenic tracer requires knowledge of the concentration and fractional solubility of that tracer in dust—estimated from measurements (McGee et al., 2016) and experiments (Baker et al., 2020).

This technique relies on knowledge of the residence time of the dissolved species at the location and depth of measurement (Equation 1). Average surface-ocean residence time can be used (Measures & Vink, 2000) but introduces uncertainty because residence times vary spatially, due largely to variation in downward particulate fluxes. Due to its predictable and well constrained production by dissolved ^{234}U, measurements of ^{230}Th enable a local residence time for ^{230}Th to be calculated from the surface to a given depth (Nozaki et al., 1981):

$$\tau_{230\_int} = \frac{\int_0^z A_{230} dz}{\lambda_{230} \int_0^z A_U dz} \quad (2)$$

where A_{230} indicates activity concentration, z is depth and λ_{230} is the decay constant for ^{230}Th. This residence time can be applied to other isotopes of thorium, so the coupled analysis of radiogenic ^{230}Th and lithogenic ^{232}Th provides a potential quantitative proxy for dust flux based only on measured ^{230}Th and ^{232}Th concentrations, half-life of ^{230}Th, and knowledge of the oceanic ^{234}U concentration.

This approach was first applied to thorium measurements in the Atlantic surface mixed-layer by Hsieh et al. (2011). However, later studies identified a ubiquitous trend of increasing calculated ^{232}Th fluxes as the depth of integration used in the calculations increases (Deng et al., 2014; Hayes et al., 2013, 2017; Hayes, Fitzsimmons, et al., 2015; Lopez et al., 2015; Pavia et al., 2020; Pérez-Tribouillier et al., 2020; Rowland et al., 2025) (Figure 1). Such apparent increases in ^{232}Th flux can be in excess of an order of magnitude and are not consistent with simple addition and dissolution of dust at the surface. Several oceanographic processes that violate the simple conceptual model have been proposed to explain this trend with depth, including vertical and lateral transport of Th by advection and diffusion, non-steady state processes, and differential partitioning between colloidal and dissolved forms (Hayes et al., 2013, 2017; Pavia et al., 2020). These processes could plausibly contribute to the apparent flux increase in the upper water column, but remain largely unproven, and do not satisfactorily explain why the apparent trend to higher Th flux with depth of integration is prevalent in diverse ocean settings ranging from high-latitude margins to remote sub-tropical gyres (Hayes et al., 2013, 2017; Pavia et al., 2020; Pérez-Tribouillier et al., 2020; Rowland et al., 2025).

Previous studies have chosen integration depths expected to best capture dust-derived signals from ^{232}Th fluxes, but the depths chosen by various authors differ. They range from the mixed layer (e.g., Hsieh et al., 2011), fixed depths of 250 or 500 m (Anderson et al., 2016; Deng et al., 2014; Hayes et al., 2013) or deep chlorophyll-maximum (Hayes et al., 2017). However, the large magnitude of the increase in the calculated ^{232}Th flux with the depth of calculation makes dust flux estimates very sensitive to the chosen depth, and there is no consensus on the most appropriate integration depth, or the origin of the depth trends. The uncertainty limits our ability to use coupled ^{232}Th and ^{230}Th measurements to make consistent quantitative assessments of dust flux.

In this study, we assess whether the ubiquitous increase in ^{232}Th flux with depth of integration could originate from the conceptual framework of the calculation method itself, rather than a violation of the model assumptions by an oceanographic process. We used modeled concentration profiles of ^{232}Th and ^{230}Th in a simple 1D framework to investigate their idealized behavior.

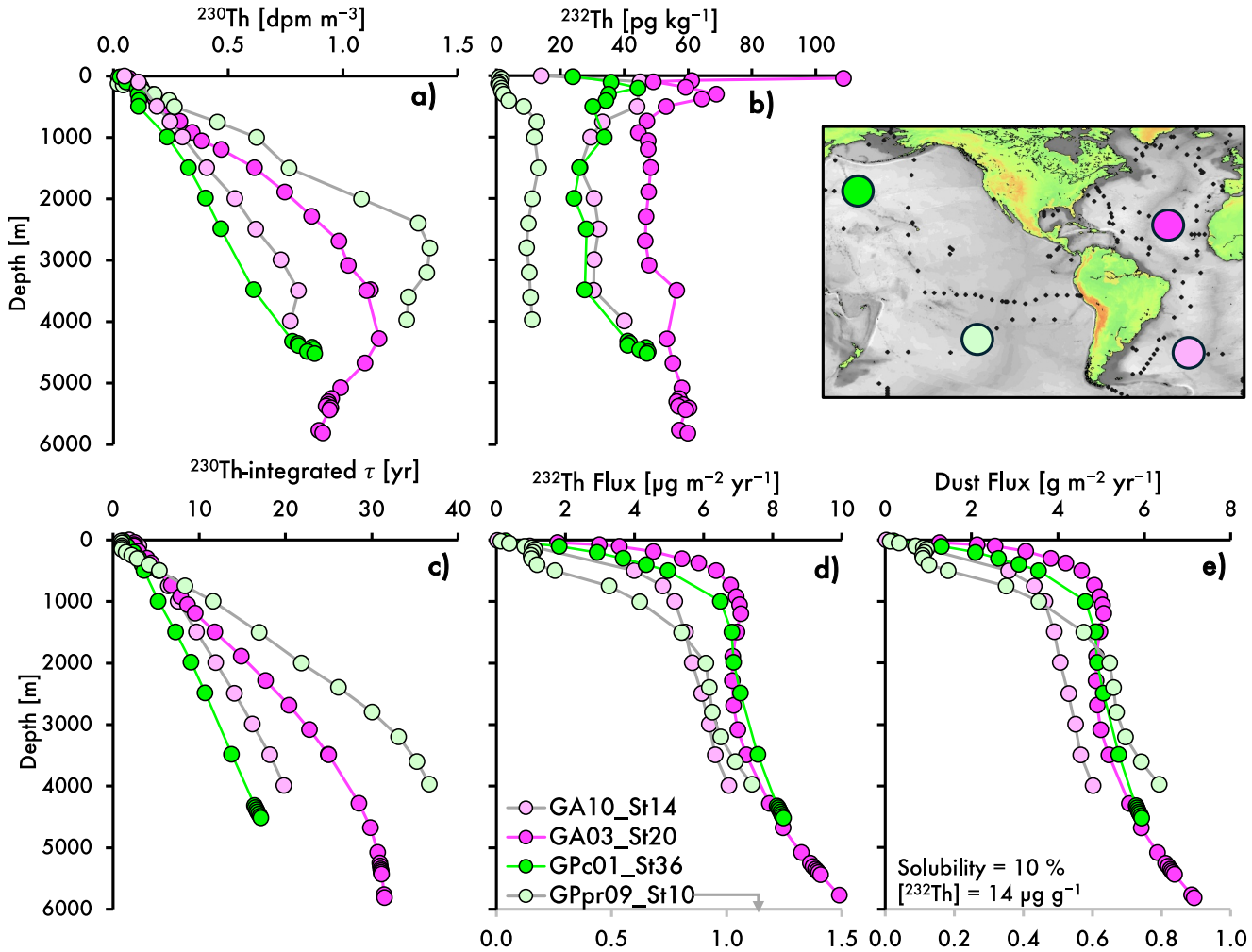

Figure 1. Examples of Th isotope data and resulting dust fluxes using the existing conceptual model. (a) Measured ^{230}Th (activity) concentration profiles in four open-ocean regions (Data from the GEOTRACES Intermediate Data Product 2021 Version 2, 2023; Hayes et al., 2013, 2018; Hayes, Anderson, et al., 2015; Schlitzer et al., 2018; Pavia et al., 2020) (b) Measured ^{232}Th concentrations for the same sites, expected to reflect predominantly atmospheric input of ^{232}Th. (c) Calculated residence time for ^{230}Th, from the surface to each sample depth. (d) Calculated downward ^{232}Th flux integrated to each sample depth, indicating the problematic apparent increase in flux with depth when using the existing conceptual model. (e) Dust flux calculated from ^{232}Th fluxes in (d), assuming a constant fractional solubility and concentration of ^{232}Th in dust (10% and 14 μg g^{-1}). Map created using Ocean Data View (Schlitzer, 2018).

2. Testing the Accuracy of Calculated ^{232}Th Fluxes in a 1-D Model

To investigate the apparent increase in ^{232}Th flux with depth of integration, we apply a simple one-dimensional reversible scavenging model (Bacon & Anderson, 1982; Nozaki et al., 1981) to derive idealized dissolved concentration profiles for each isotope from prescribed source terms and with typical values for variables involved in ocean particle cycling. Using the resulting idealized profiles of ^{230}Th and ^{232}Th from this model, we test if Equations 1 and 2, commonly used to calculate dust flux from ocean observations, can correctly reproduce the prescribed ^{232}Th flux.

2.1. Sources of ^{230}Th and ^{232}Th

Thorium-230 in the ocean exists in two pools: as an adsorbed phase on particle surfaces, and dissolved in seawater (operationally defined as passing through a filter of a given pore size, commonly 0.45 or 0.2 μm). Thorium-232 is thought to share this partitioning but also exists in a lattice-bound form in lithogenic particles (e.g., dust), from which it can dissolve and move into the adsorbed particulate or dissolved phases. In this study, we focus on describing and modeling the dissolved pool of each isotope, which is inherently linked to the adsorbed particulate

phase through reversible scavenging (Bacon & Anderson, 1982). In the remainder of the paper, reference to ^{230}Th or ^{232}Th indicates the dissolved form of the isotope.

Although ^{230}Th and ^{232}Th share the same removal processes in the ocean—adsorption to sinking particles— the two isotopes have very different concentration profiles due to their different sources (Figures 1a and 1b). Profiles of ^{230}Th generally increase linearly through the water column from low surface values due to constant seawater production of ^{230}Th by the radioactive decay of dissolved ^{234}U and continuous cycles of adsorption–desorption between dissolved Th and sinking particles (Bacon & Anderson, 1982). In contrast, the partial dissolution of lithogenic particles—transported to the ocean by wind, rivers and in nepheloid layers—supplies ^{232}Th to the ocean in a spatially heterogeneous pattern. In the remote open-ocean, far from other sources, the dominant source of ^{232}Th is thought to be the dissolution of aeolian dust near the surface, resulting in ^{232}Th profiles that show relatively little variation with depth below the upper ~1,000 m (Figure 1b). In this study, we focus on modeling these remote settings, ignoring additional processes that can supply ^{232}Th nearer the ocean margins. The same reversible exchange between adsorbed and dissolved forms of Th communicates the surface ^{232}Th signal to depth by particle settling.

2.2. Reversible Scavenging Model

Reversible scavenging models were developed to explain linearly increasing profiles of particulate ^{230}Th and dissolved ^{230}Th. Away from regions of significant ventilation, the model describes ^{230}Th observations well (Bacon & Anderson, 1982; Moran et al., 2002; Nozaki et al., 1981; Roy-Barman et al., 1996). Linear profiles of ^{230}Th emerge as supply at each depth depends on the integrated production in the overlying water column. Cycles of adsorption and desorption to and from sinking particles transport Th to deeper waters (Equation 3). The dissolved ^{230}Th concentrations (A_{230_d}) are therefore related to the rate constants of adsorption (k_1) and desorption (k_{-1}), the particle settling rate (S), in situ production by ^{234}U (P_{230}; fixed constant) and the integrated production in the overlying water column ($\lambda_{230}\int_0^z A_U dz \approx P_{230}z$).

$$A_{230\_d} = \frac{P_{230}}{k_1} + \frac{k_{-1}P_{230}z}{k_1 S} \tag{3}$$

This equation is used to calculate ^{230}Th concentrations at depths from 0 to 6,000 m in an idealized water column (Figure 2a). All parameters used in this model are described, with their units and values in Table 1. We assume that the rate constants, settling rate and ^{230}Th production are constant with depth and that fluxes due to advection, diffusion and radioactive decay of ^{230}Th are zero. This calculation returns non-zero ^{230}Th at the surface (i.e., $z = 0$), matching observations (Figure 1).

The integrated residence time for dissolved ^{230}Th from the surface to the depth, z, can be calculated in the model (from its prescribed values for k_1, k_{-1}, and S) from the following equation:

$$\tau_{230\_\mathrm{int}} = \frac{1}{k_1} + \frac{k_{-1}z}{k_1 S}\cdot\frac{1}{2} \tag{4}$$

The first term represents the partial residence time due to adsorption onto particles and the second term relates to the average time for removal of dissolved ^{230}Th by sinking particles at the given integration depth (Nozaki et al., 1981). The factor of ½ exists because ^{230}Th is produced equally at all depths, so the average distance settled by ^{230}Th adsorbed to particles is half the integration depth (Nozaki et al., 1981).

A similar pair of equations can be written for ^{232}Th, which differ only in the source term, P_{232}, reflecting the dissolution of ^{232}Th from dust. These equations highlight that the integrated residence time of each isotope in the model depends on the spatial distribution of the supply term ($P_{232,\ 230}$) with depth (i.e., the integral and double integral in Equation 6)

$$A_{232\_d} = \frac{P_{232}}{k_1} + \frac{k_{-1}\int_0^z P_{232}dz}{k_1 S} \tag{5}$$

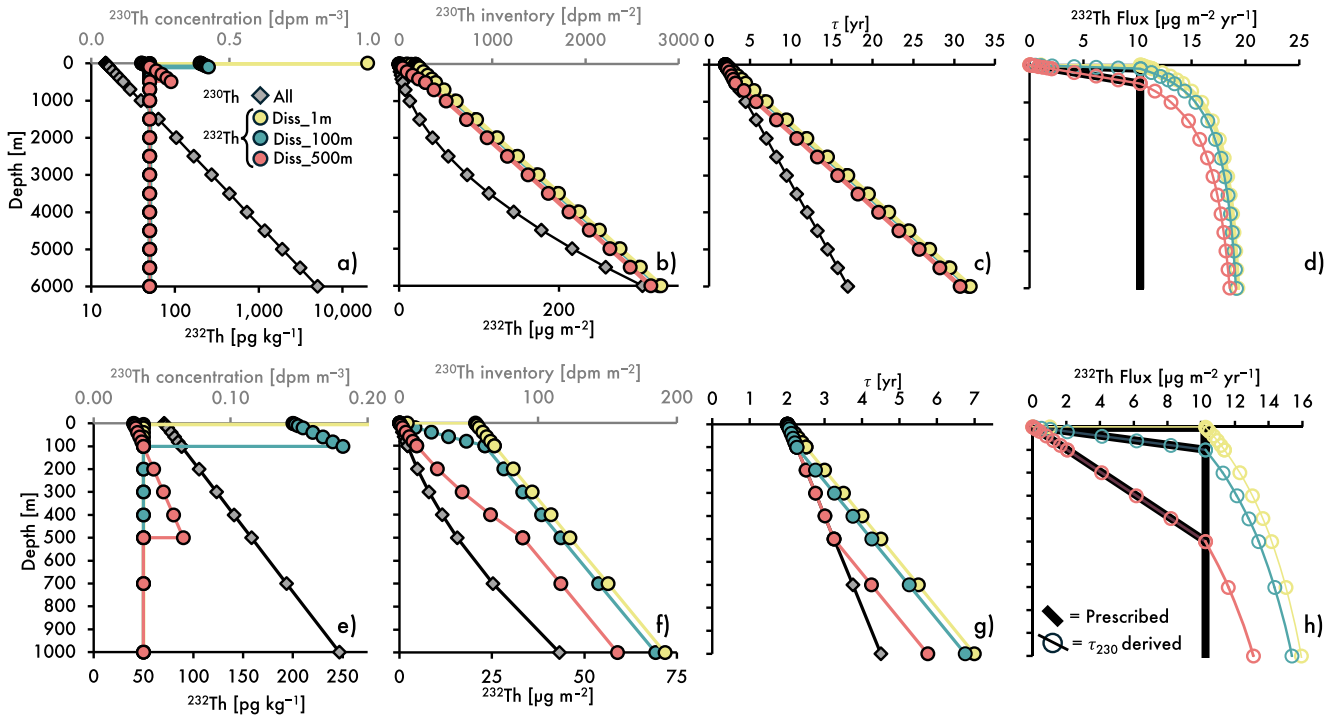

Figure 2. Water column profiles from the 1-D scavenging model for three model scenarios: Diss_1m, Diss_100m, Diss_500m. (a, e) Modeled concentrations of ^{230}Th (gray diamonds, upper axis) and ^{232}Th (colored circles, lower axis). (b, f) ^{230}Th and ^{232}Th inventories. (c, g) Integrated residence time for ^{230}Th and ^{232}Th. (d, h) Modeled ^{232}Th flux profiles estimated from ^{230}Th residence time (open circles) and prescribed model input (black lines).

$$\tau_{232\_int} = \frac{\int_0^z A_{232}dz}{\int_0^z P_{232}dz} = \frac{1}{k_1} + \frac{k_{-1}\int_0^z \int_0^z P_{232}dz\,dz}{Sk_1 \int_0^z P_{232}dz} \quad (6)$$

Table 1
Parameters Used in the Reversible Scavenging Model

Scenario	Symbol	Values	Description/analytical solution	Type	Source/Reference
All	$\int_0^z P_{232}dz$	10.25 [μg m^{-2} yr^{-1}][a]	^{232}Th production flux	Prescribed	Atlantic ^{232}Th measurements (Hayes et al., 2018; Moran et al., 2002; Rowland et al., 2017)
All	S	800 [m yr^{-1}]	Particle settling rate	Constant	N. Atlantic particulate ^{230}Th (Anderson et al., 2016)
	k_1	0.5 [yr^{-1}]	Adsorption rate	Constant	Dissolved and particulate ^{234,230}Th (Bacon & Anderson, 1982; Lerner et al., 2017)
	k_{-1}	2 [yr^{-1}]	Desorption rate	Constant	
	P_{230}	0.0256 [dpm m^{-3} yr^{-1}][b]	^{230}Th production rate: $A_U\lambda_{230}$	Constant	Uranium–salinity relationship (Andersen et al., 2010; Costa et al., 2020; Owens et al., 2011)
All	A_{230_d}	0.05–0.82 [dpm m^{-3}] (z = 0–6,000 m)	Dissolved ^{230}Th: $\frac{P_{230}}{k_1} + \frac{k_{-1}\int_0^z P_{230}dz}{Sk_1}$	Modeled	Reversible scavenging model (Bacon & Anderson, 1982)
	A_{230_p}	0–0.19 [dpm m^{-3}] (z = 0–6,000 m)	Particulate ^{230}Th: $\frac{P_{230}z}{S}$	Modeled	
	A_{232_d}	50–250 [pg kg^{-1}] (z = 0–6,000 m)	Dissolved ^{232}Th: $\frac{P_{232}}{k_1} + \frac{k_{-1}\int_0^z P_{232}dz}{Sk_1}$	Modeled	

[a]Integrated ^{232}Th flux is assumed to be released over three different depth ranges in separate model scenarios, as described in the text. [b]Calculated assuming salinity–^{238}U relationship of Owens et al. (2011) with salinity = 35 and ^{234}U/^{238}U activity ratio of 1.1467.

We use Equation 5 to calculate the idealized profile of ^{232}Th with water depth based on prescribed variables (Table 1). We do this for three cases in which the dust is assumed to release ^{232}Th into the water over three depth ranges:

- **Diss_1m**: All ^{232}Th is produced by release from dust only in the uppermost 1 m of the water column
- **Diss_100m**: ^{232}Th is released uniformly over the upper 100 m, and not below
- **Diss_500m**: ^{232}Th is released uniformly over the upper 500 m, and not below.

In all three cases, the total ^{232}Th released is 10.25 μg m^{-2} yr^{-1} (Table 1).

Note that the different depths over which ^{232}Th is assumed to be produced by dust release lead to very different expected ^{232}Th concentrations in near-surface waters (Figure 2a). This reflects the magnitude of the first term (P_{232}/k_1) in Equation 5. Below this depth, in the absence of further ^{232}Th production, the model ^{232}Th concentrations are constant with depth at the same value in all three model cases. These features of the modeled ^{232}Th are compared to observations in Section 3 below.

We next calculate residence times for ^{230}Th and ^{232}Th. The former can be calculated from the model parameters (e.g., Equation 4) or from the measured values used when calculating fluxes in the field (Equation 2); these approaches give identical residence times for ^{230}Th. The ^{232}Th residence time is calculated from Equation 6.

2.3. Accuracy of ^{232}Th Fluxes Derived From ^{230}Th Residence Times

The model ^{232}Th profiles, calculated as they are from a prescribed ^{232}Th flux and idealized scenario, can be used to assess the ability of calculations using water-column Th observations to derive an accurate ^{232}Th flux (i.e., ^{232}Th fluxes calculated using Equations 2 and 4 can be compared to those prescribed).

In all three model scenarios ^{230}Th-calculated ^{232}Th fluxes faithfully reproduce the prescribed flux in the upper water-column, down to the depth at which dissolution of dust is assumed to cease (1 m, 100 m or 500 m) (Figures 2d and 2h). Below these depths, however, the calculated ^{232}Th flux increases, rather than remaining constant as prescribed, to over-estimate ^{232}Th fluxes by a factor that approaches 2 at the greatest depths. The depth profile of calculated ^{232}Th fluxes therefore shows a pattern of significant increase with depth, similar to that seen in observational studies (e.g., Figure 1).

Near the surface, the increase in calculated ^{232}Th flux reflects a real (i.e., prescribed) increase in flux generated by progressive dissolution of dust and release of ^{232}Th to the dissolved phase over a depth range in the ocean.

At greater depths, the further increase in ^{232}Th flux is not a good reflection of prescribed values, and tends toward fluxes twice as high as those prescribed. The factor of two errors can be explained by the different profiles of addition of the two thorium isotopes and therefore their different integrated residence times (Nozaki et al., 1981). Because ^{230}Th is produced equally throughout the integrated layer, the average depth ^{230}Th must be transported downwards by particles to leave the layer is ½ the depth of integration (Nozaki et al., 1981). As depth increases, the $1/k_1$ term in Equation 4 becomes increasingly insignificant and τ_{230_int} tends to $\frac{k_{-1}z}{k_1 S}\cdot\frac{1}{2}$. In contrast, ^{232}Th is produced only near the surface, and so must transit almost the whole integrated layer so that $\tau_{232\_int} \approx \frac{k_{-1}z}{k_1 S}$. Hence, at large depths, the ^{232}Th fluxes calculated from ^{230}Th residence time using field measurements and Equation 2 are overestimated by a factor approaching 2 times (Figures 2 and 3).

The implication of our analysis is that the conceptual framework used previously to calculate dust fluxes from thorium measurements (e.g., Equation 2; Anderson et al., 2016; Hayes et al., 2013; Hsieh et al., 2011; Pavia et al., 2020) may be appropriate in the depth range where dust dissolution occurs, but it overestimates ^{232}Th fluxes at greater depths by a factor of two. Because the integrated ^{230}Th residence times reflect a balance between shallow values, where the adsorption timescale dominates, and deep values where the settling timescale dominates (Equation 4), there is no simple correction factor that can readily be applied to correct ^{230}Th residence times at all depths to give accurate ^{232}Th fluxes.

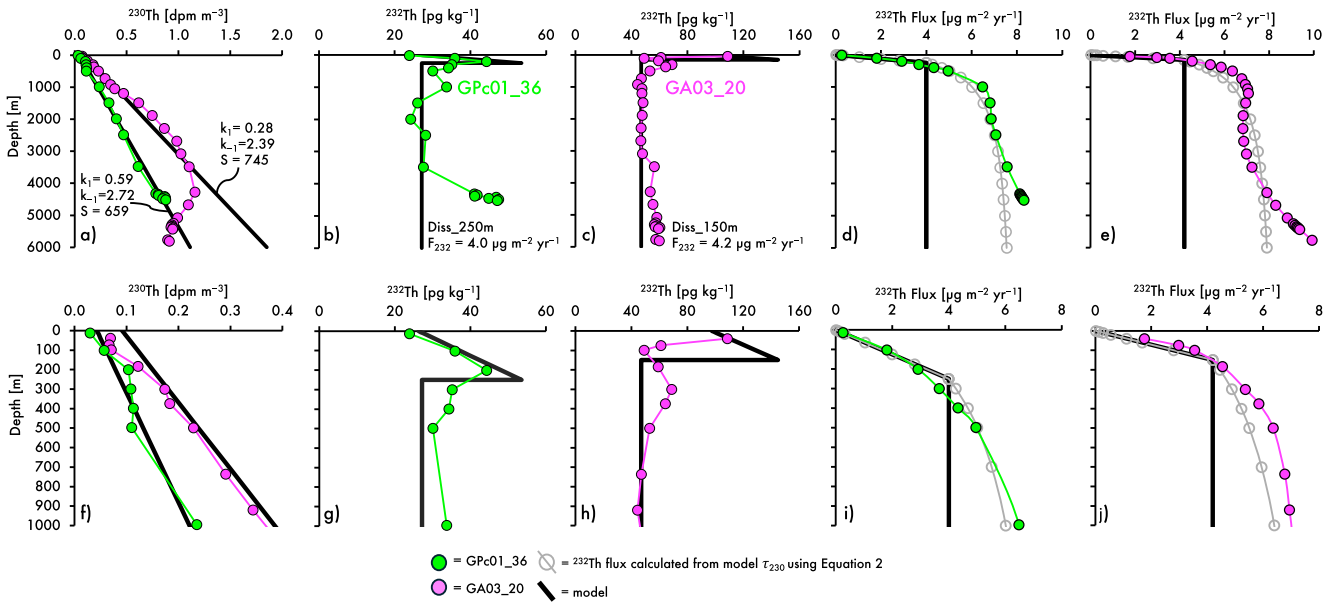

Figure 3. Reversible scavenging model tuned to thorium measurements from two ocean stations to demonstrate release of ^{232}Th from dust in the near surface, and over-estimate of ^{232}Th flux in deeper waters when using traditional ^{230}Th residence times. (a, f) Model ^{230}Th profiles (black lines) tuned to two measured profiles (GA03_20, magenta; GPc01_36, green). (b, c, g, h) Model ^{232}Th profiles to fit GPc01_36 (b, g; ^{232}Th flux = 4.0 μg m^{-2} yr^{-1} over 250 m) and GA03_20 (c, h; ^{232}Th flux = 4.2 μg m^{-2} yr^{-1} over 150 m). (d, e, i, j) Thorium-232 flux model profiles calculated from model data using traditional ^{230}Th residence times (gray open circles), and compared to field data calculated in the same way, and to the actual ^{232}Th flux in the model (black line).

3. Comparison of Modeled and Observed Th Isotope Profiles

By altering the parameters in the model, we can match the observed profiles of ^{230}Th and ^{232}Th and assess the downward flux of ^{232}Th and the depth of dust dissolution that best explains these profiles. We do this for two example locations, one each from the Atlantic and Pacific (Figure 3).

We tuned S, k_1, and k_{-1} to give a good fit to the ^{230}Th profile at the two sites, and then used these site-specific values to model ^{232}Th at each site (Figures 2a and 2f). We then adjusted the maximum depth of dust dissolution and the total flux of added ^{232}Th to give a reasonable fit to the observed ^{232}Th profiles (Figures 2b, 2c, 2g, and 2h). It is noteworthy that at both these sites, and in many other field sites, high values of ^{232}Th are observed in the upper few 100 m of the water column, which is consistent with the release of ^{232}Th from dust as it settles in the upper water column.

In contrast, if ^{232}Th release actually occurs only at the very surface, the model predicts extremely high ^{232}Th concentrations at the surface (i.e., **Diss_1m**; Figure 2a). Since these high values are not generally observed, all dissolution cannot occur at the surface, or additional processes outside of our model framework, such as diffusion or changing adsorption rates, are required to explain the measured ^{232}Th concentration profiles. Because these additional processes would also impact ^{230}Th distributions (which are modeled reasonably well without them), we consider ^{232}Th release over a given depth range as the simplest scenario by which realistic ^{232}Th concentration profiles can be produced. This approach of fitting observed profiles with the 1-D scavenging model indicates that while ^{232}Th fluxes derived from ^{230}Th measurements using existing approaches may be accurate near the surface, they are systematically too high at greater depths.

As outlined by previous studies (e.g., Pavia et al., 2020), physical mechanisms such as vertical mixing may also impact apparent ^{232}Th fluxes calculated from measurements. If additional ^{230}Th is supplied to the shallow ocean by vertical mixing, residence times will be overestimated and ^{232}Th fluxes will be underestimated at these depths, potentially accounting for low ^{232}Th fluxes near the surface. The impact on ^{232}Th fluxes is also dependent on the sign of the ^{232}Th gradient, which may accentuate or diminish the effect from ^{230}Th. A simple calculation considering only ^{230}Th suggests that in realistic mixing scenarios, the impact of mixing on residence time biases is small (decreasing with depth from ≤10% at ∼100 m), so this process is unlikely to explain increasing ^{232}Th fluxes (Figure S1; Figure 3g).

4. An Alternative Approach for Assessing ^{232}Th Fluxes to the Ocean

4.1. Alternative ^{232}Th Residence Time Estimates

The model shows that ^{232}Th fluxes calculated from observed ^{230}Th residence times (using Equations 1 and 2) become progressively more biased with increasing integration depth. Most studies using the ^{232}Th-^{230}Th method to calculate dust inputs have used limited integration depths (~25–500 m) to provide a local assessment of dust flux and avoid the impact of advected signals, including of non-dust lithogenic input from ocean margins (Anderson et al., 2016; Deng et al., 2014; Hayes et al., 2013, 2017; Hsieh et al., 2011; Pavia et al., 2020), although some studies have presented depth profiles of ^{232}Th fluxes extending to well below the surface (Hayes et al., 2013, 2018; Hayes, Fitzsimmons, et al., 2015; Pérez-Tribouillier et al., 2020; Rowland et al., 2025). If there is a requirement to capture total dust dissolution, it may be preferable to integrate ^{232}Th to greater depths to capture the whole dissolution process. In such cases, we suggest an alternative approach for estimating ^{232}Th fluxes at greater depths that better matches the true ^{232}Th fluxes.

For our model, below the last depth that ^{232}Th is produced, Z_{LP}, the correct equation for ^{232}Th residence time can be expressed as shown in Equation 7 (derived from Equation 6):

$$\tau_{232,Z>Z_{LP}} = \frac{1}{k_1} + \frac{k_{-1}\left(z - \frac{z_{LP}}{2}\right)}{k_1 S} \tag{7}$$

When $z \gg z_{LP}$ this equation approximates to:

$$\tau_{232,Z\gg Z_{LP}} \approx \frac{1}{k_1} + \frac{k_{-1} z}{k_1 S} \tag{8}$$

The ^{232}Th residence time calculated from Equation 8 is approximately equivalent to the in situ ^{230}Th residence time, that is, the ^{230}Th residence time if production and concentration terms *are not* integrated but calculated for a specific depth. We term this the "volumetric" residence time because parameters contain units of m^{-3}. It can be considered the residence time of ^{230}Th due to in situ radiogenic production at a given depth, that is, the amount of ^{230}Th in a volume divided by the input flux of ^{230}Th by ^{234}U decay in the same volume (Equation 9).

$$\tau_{230\_vol}[\mathrm{yr}] = \frac{A_{230_d}}{\lambda_{230} A_U} = \frac{A_{230_d}}{P_{230}} \frac{[\mathrm{dpm\ m^{-3}}]}{[\mathrm{dpm\ m^{-3}\ yr^{-1}}]} \tag{9}$$

This residence time can be calculated from ^{230}Th measurements in the ocean at any depth, and this timescale can be applied to integrated ^{232}Th inventories at the same depth to produce an integrated ^{232}Th flux estimate (Equation 1).

This new approach to calculating ^{230}Th residence times provides a method to assess ^{232}Th fluxes from field measured ^{230}Th and ^{232}Th concentrations which, at greater water depths, is significantly more accurate than the integrated approach used in previous studies. Applying the volumetric approach to modeled data gives an estimate of ^{232}Th flux that closely approaches the prescribed ^{232}Th flux (Figure 4). For example, the volumetric residence time underestimates the prescribed ^{232}Th fluxes by a maximum of 10% at 100 m for **Diss_100m**, and 28% at 500 m for **Diss_500m**, and is more accurate than integrated ^{230}Th-derived ^{232}Th fluxes at depths of ~200 and ~850 m, respectively.

4.2. Recommended Approaches for Calculating ^{232}Th Flux

In this section, we consider two approaches to calculate accurate ^{232}Th flux estimates from ^{230}Th–^{232}Th observations in shallow and deep parts of the water column.

4.2.1. Shallow ^{232}Th Fluxes

Near the surface, where increased ^{232}Th concentrations indicate release of ^{232}Th from dust, integrated ^{230}Th residence times, as used in previous studies (Equation 2), are expected to give a reasonable assessment of actual

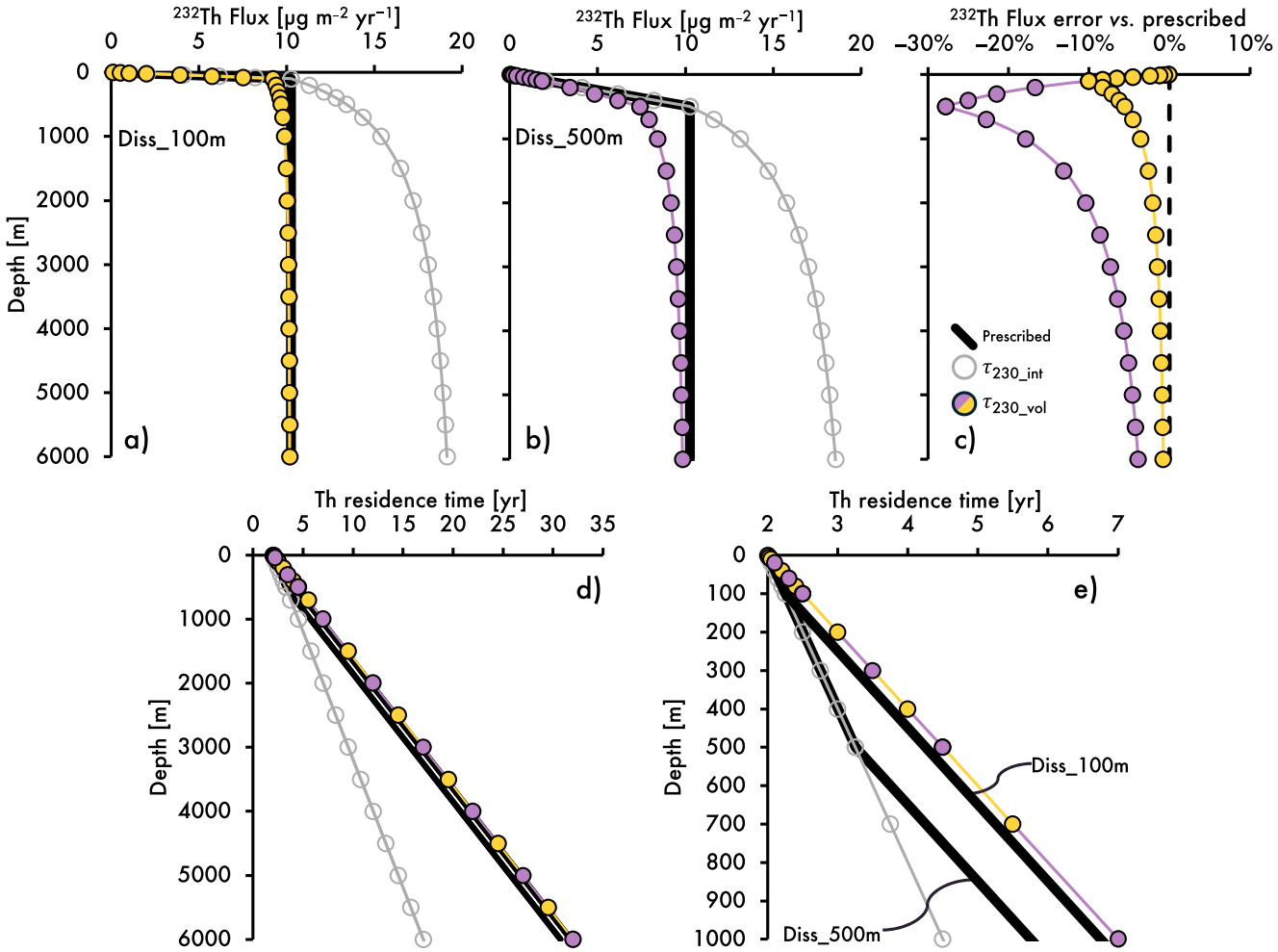

Figure 4. Comparison of calculated ^{232}Th fluxes with actual fluxes, using the traditional integrated approach and our new volumetric approach. (a and b) ^{232}Th fluxes calculated using ^{230}Th residence times integrated to depth (open circles) and volumetrically at each depth (filled circles), compared to prescribed fluxes (black lines) for model Diss_100m and Diss_500m, respectively. (c) Percentage difference of ^{232}Th fluxes calculated with the volumetric approach from prescribed fluxes. (d, e) Residence times corresponding to ^{232}Th flux estimates in (a, b). Thorium-230 derived residence times are identical in both model scenarios.

^{232}Th fluxes. There is, however, remaining uncertainty about the profile of ^{232}Th release from dust with depth at any given site; whether it is uniform with depth, and the depth at which it ceases.

For studies investigating nutrient supply to phytoplankton, where it is important to capture the trace-metal supply to the depth where plankton live, an approach previously suggested (Hayes et al., 2017) is to integrate nutrient supply into the base of the deep chlorophyll maximum. Our model suggests this is valid, provided ^{232}Th concentration profiles increase to this depth, which would be indicative of dust dissolution and reversible scavenging occurring over this depth range. Any dust dissolution that occurs below this depth would be considered less relevant for supplying nutrients to contemporaneous plankton. However, continuing to apply the integrated ^{230}Th residence time too deep in the water column risks overestimation of ^{232}Th flux (Figures 3d, 3e, and 4) and identifying the point at which dust is no longer releasing ^{232}Th may not be trivial. The risk of overestimating ^{232}Th fluxes can be minimized by applying the volumetric ^{230}Th residence time (Equation 9), as the values are likely to be close to the correct Th residence time in the shallow water column (Figure 4) and closely reflect the accurate residence time of ^{232}Th at larger depths.

4.2.2. Deep ^{232}Th Fluxes

If the total dust flux to the ocean, rather than nutrient flux to plankton, is the parameter of interest, the depth at which ^{232}Th concentrations reach their maximum in the upper ~1,000 m can be used to infer the end of ^{232}Th

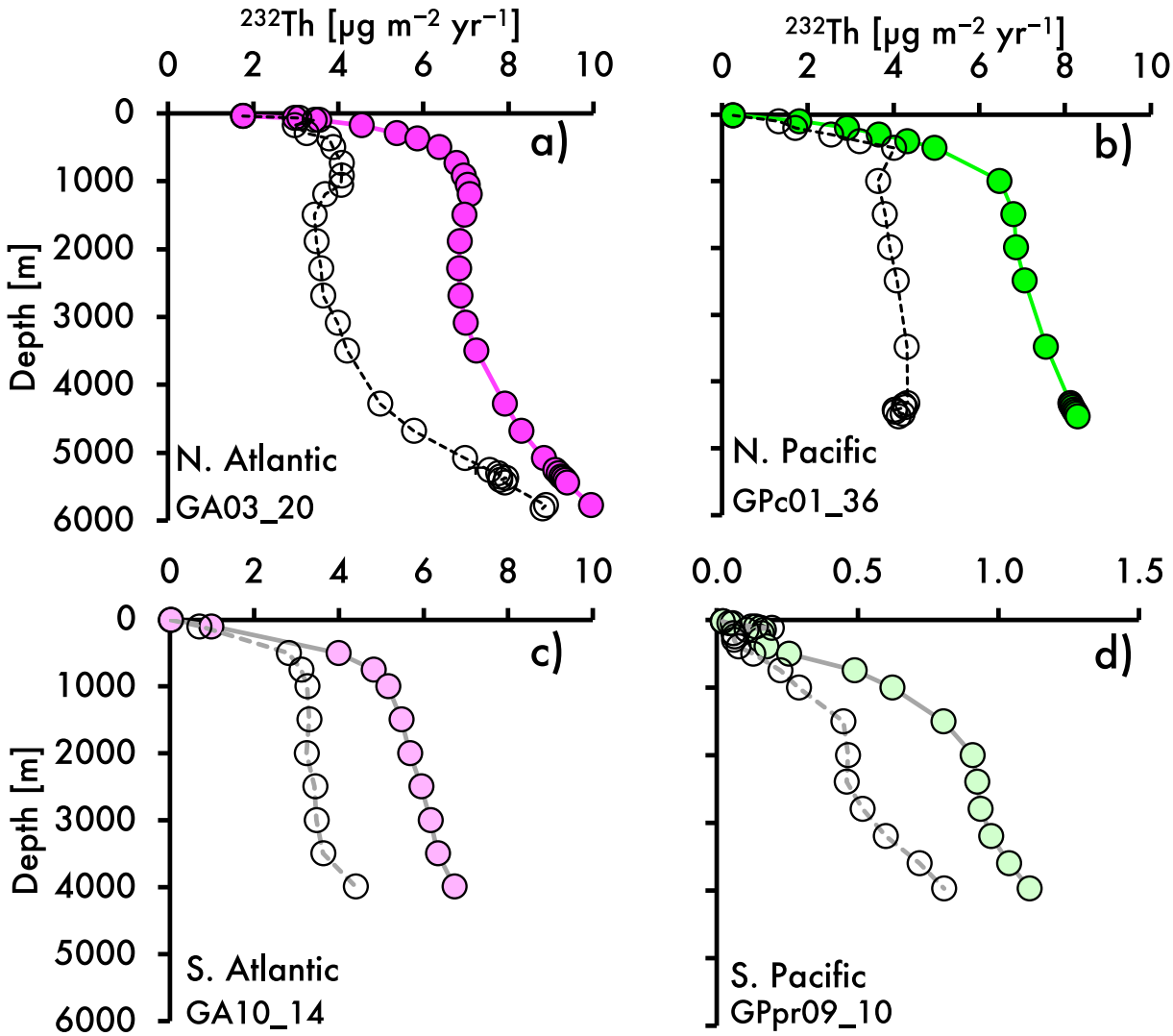

Figure 5. GEOTRACES ^{232}Th flux profiles calculated using previously used integrated ^{230}Th residence times (solid symbols; identical to those shown in Figure 1d) and the volumetric ^{230}Th residence suggested in this study. Note that the integrated approach yields values that 1.2–2.0 higher than the volumetric at 500 m, and 1.8–2.0 higher at 2,000 m, and are considered overestimates of the true downward flux of ^{232}Th.

production by dust dissolution (Figure 1b). Below this depth, ^{232}Th fluxes calculated using volumetric ^{230}Th residence times become reasonably constant (Figures 4 and 5a–5c), consistent with limited further ^{232}Th production. We suggest that for flux profiles that fit with our simplified model of ^{232}Th cycling (Figures 3 and 5a–5c), water depths of 1,000–3,000 m can provide an accurate estimate of ^{232}Th flux when using our revised volumetric ^{230}Th residence time (Equation 9). At this depth range, there is more potential for lateral movement of ^{232}Th, so the dust flux is likely to be averaged over the local region, and care should be taken in proximity to ocean margins, but in the open ocean, this approach is expected to give reliable dust fluxes from combined ^{230}Th–^{232}Th measurements. At greater depths, the problem of lateral movement will become more acute and ^{232}Th signals due to resuspension near the seafloor may also become a problem (e.g., Figure 1b). Thorium-232 concentrations that are constant with depth provide an initial indication that the cycling in the deep water column fits with our conceptual model (Figure 1).

To demonstrate this for real measurements, we processed the ^{230}Th and ^{232}Th profiles shown in Figure 1 using the volumetric approach (Equation 9).

Example profiles from the Pacific and Atlantic are shown in Figure 5. In the North Atlantic and North Pacific, ^{232}Th fluxes calculated using the volumetric approach increase to a maximum of ∼4 μg m^{-2} yr^{-1} by ∼500 and

100 m, respectively, but remain close to this value for the next several thousand meters, consistent with no further ^{232}Th production, and more in line with expectations for downward ^{232}Th fluxes than fluxes calculated with previously used approaches (Figures 3d and 3e; Equation 2).

In reality, ^{232}Th concentration profile shapes are variable (e.g., Figure 1b) and do not perfectly agree with the simple model scenario outlined here. The increases in ^{232}Th flux at greater depths seen in some regions (Figures 5a and 5d) can be linked to processes that violate model assumptions (e.g., due to presence of recently ventilated low-^{230}Th bearing waters the deep North Atlantic; Moran et al., 2002), leading to apparent reductions in the ^{230}Th residence times and the apparent increases in ^{232}Th fluxes (Figure 5a). Such processes must still be considered when applying ^{230}Th residence times to calculate ^{232}Th fluxes, even with our revised methodology. We highlight that ^{232}Th and dust flux estimates may not be reliable where ^{232}Th concentration profiles deviate significantly from those that are predicted by the simple model of near-surface dust addition. For example, because the true ^{232}Th residence time depends on the spatial pattern of the ^{232}Th source term, processes that supply ^{232}Th below the surface—such as nepheloid layers—will also impact the accuracy of ^{232}Th fluxes derived from ^{230}Th residence times, including those calculated using our revised methodology. The ^{232}Th concentration profiles should be evaluated for consistency with the conceptual model before the data are used to infer dust fluxes.

4.2.3. Reinterpreting ^{232}Th and Dust Flux Estimates

Thorium-232 fluxes calculated using integrated ^{230}Th residence times are already larger than our revised estimates by 1.4–2.4 times at ∼250 and ∼500 m for the four example profiles (Figure 5), suggesting that significant bias is possible even in the shallower depth range that is usually integrated (∼250–500 m; Anderson et al., 2016; Deng et al., 2014; Hayes et al., 2013, 2017; Hsieh et al., 2011; Pavia et al., 2020). There may be further implications for studies that have interpreted full-depth ^{232}Th flux profiles, as these are more likely to be biased high (e.g., Hayes et al., 2018), as well as for comparison between dissolved ^{232}Th fluxes and ^{230}Th-normalized particulate ^{232}Th fluxes (Anderson et al., 2016; Pavia et al., 2020). Calculating sedimentation rates and fluxes of elements (including of ^{232}Th) to marine sediments is commonly achieved using ^{230}Th-normalization, which relies on quantitative removal of all ^{230}Th produced in the overlying water column to the sediment. This normalization approach is not influenced by the difference in addition profiles in the water column for ^{230}Th and ^{232}Th. Thorium-232 is within or adsorbed to the same particles that remove ^{230}Th, and the sediment is integrating the whole water-column, so ^{230}Th-normalized ^{232}Th fluxes are expected to reflect the true ^{232}Th flux, despite differences in the integrated residence times of the dissolved isotopes in the overlying water column.

For station GA03_20 at ∼2,000 m, dissolved ^{232}Th fluxes fall from 60% of the total particulate ^{230}Th-normalized ^{232}Th flux using the integrated ^{230}Th method (∼11 μg m^{-2} yr^{-1}; Anderson et al., 2016), to ∼30% using our revised method, which is more in line with nearby sediment-seawater ^{232}Th/^{230}Th comparisons (Rowland et al., 2017). Similarly, at station GPpr09_10 (Pavia et al., 2020), between 1,000 and 3,000 m, dissolved ^{232}Th fluxes calculated using the integrated ^{230}Th residence time are actually higher than particulate ^{230}Th-normalized ^{232}Th fluxes (by 16%–67%); using the revised method lowers the dissolved fluxes to ∼75% of the ^{230}Th-normalized particulate values. Although these revised dissolved ^{232}Th fluxes are still a high proportion of the particulate ^{232}Th flux, they are much more in-line with expected thorium behavior (i.e., that more of the total ^{232}Th flux would be carried within lithogenic particles compared to the dissolved phase).

5. Conclusions

Using a simple 1-D reversible scavenging model for ^{230}Th and ^{232}Th, we have analyzed the origin of increases in apparent ^{232}Th fluxes seen in previous studies using measurements of ^{232}Th and ^{230}Th in seawater. Our modeling indicates that the existing method for estimating ^{232}Th residence time, using ^{230}Th residence times integrated from the surface to a given depth, leads to overestimation of ^{232}Th fluxes tending to a factor of 2 with depth. This arises as the integrated ^{230}Th residence time depends, in part, on the average time particles spend settling through the integrated layer (due to constant ^{230}Th production at all depths), whereas for ^{232}Th the residence time reflects the total time for particles to settle through the whole integrated layer.

In the upper few hundred meters of the water column, the model indicates that the higher observed ^{232}Th concentrations are likely to reflect progressive release of ^{232}Th from dust as particles settle. In this depth range, both ^{230}Th and ^{232}Th may be produced constantly with depth and ^{230}Th integrated residence times accurately reflect

^{232}Th residence times. However, because of the different sources of each isotope—dissolved uranium and lithogenic material—this situation is more likely to be the exception, rather than the rule in much of the rest of the water column.

We have shown that an alternative formulation of ^{230}Th residence time can provide an estimate of ^{232}Th residence time that gives a close approximation to the true ^{232}Th flux, particularly for deeper waters. We show that some previous ^{232}Th flux estimates are likely to be overestimated by up to a factor of ∼2.

This study indicates that ^{230}Th and ^{232}Th concentration profiles should be scrutinized for consistency with the reversible scavenging model; integrated ^{230}Th residence times should only be applied at shallower integration depths where it can be confirmed that both isotopes share similar cycling. Using our revised estimate of ^{232}Th residence time provides a more accurate approach to integrate to larger depths, capturing the total dissolution of ^{232}Th from dust and removing the bias found in the existing method.

Conflict of Interest

The authors declare no conflicts of interest relevant to this study.

Availability Statement

All data on which this study is based can be found at https://doi.org/10.5281/zenodo.18343942 (Rowland & Henderson, 2026).

Acknowledgments
The authors acknowledge funding from the Natural Environment Research Council (NERC) (Grant NE/V001213/1).

References

Andersen, M. B., Stirling, C. H., Zimmermann, B., & Halliday, A. N. (2010). Precise determination of the open ocean ^{234}U/^{238}U composition. *Geochemistry, Geophysics, Geosystems*, *11*(12), 12003. https://doi.org/10.1029/2010GC003318

Anderson, R. F., Cheng, H., Edwards, R. L., Fleisher, M. Q., Hayes, C. T., Huang, K.-F. F., et al. (2016). How well can we quantify dust deposition to the ocean? *Philosophical Transactions of the Royal Society A: Mathematical, Physical and Engineering Sciences*, *374*(2081), 20150285. https://doi.org/10.1098/rsta.2015.0285

Bacon, M. P., & Anderson, R. F. (1982). Distribution of thorium isotopes between dissolved and particulate forms in the deep sea. *Journal of Geophysical Research*, *87*(C3), 2045–2056. https://doi.org/10.1029/jc087ic03p02045

Baker, A. R., Li, M., & Chance, R. (2020). Trace metal fractional solubility in size-segregated aerosols from the tropical eastern Atlantic Ocean. *Global Biogeochemical Cycles*, *34*(6), e2019GB006510. https://doi.org/10.1002/essoar.10501469.1

Buchanan, P. J., Chase, Z., Matear, R. J., Phipps, S. J., & Bindoff, N. L. (2019). Marine nitrogen fixers mediate a low latitude pathway for atmospheric CO_2 drawdown. *Nature Communications*, *10*(1), 4611. https://doi.org/10.1038/s41467-019-12549-z

Costa, K. M., Hayes, C. T., Anderson, R. F., Pavia, F. J., Bausch, A., Deng, F., et al. (2020). ^{230}Th normalization: New insights on an essential tool for quantifying sedimentary fluxes in the modern and Quaternary ocean. *Paleoceanography and Paleoclimatology*, *35*(2), e2019PA003820. https://doi.org/10.1029/2019PA003820

Deng, F., Thomas, A. L., Rijkenberg, M. J. A., & Henderson, G. M. (2014). Controls on seawater ^{231}Pa, ^{230}Th and ^{232}Th concentrations along the flow paths of deep waters in the Southwest Atlantic. *Earth and Planetary Science Letters*, *390*, 93–102. https://doi.org/10.1016/j.epsl.2013.12.038

GEOTRACES Intermediate Data Product Group. (2023). The GEOTRACES intermediate data product 2021v2 (IDP2021v2) [Dataset]. *NERC EDS British Oceanographic Data Centre NOC*. https://doi.org/10.5285/ff46f034-f47c-05f9-e053-6c86abc0dc7e

Hamilton, D. S., Moore, J. K., Arneth, A., Bond, T. C., Carslaw, K. S., Hantson, S., et al. (2020). Impact of changes to the atmospheric soluble iron deposition flux on ocean biogeochemical cycles in the Anthropocene. *Global Biogeochemical Cycles*, *34*(3), e2019GB006448. https://doi.org/10.1029/2019GB006448

Hayes, C. T., Anderson, R. F., Cheng, H., Conway, T. M., Edwards, R. L., Fleisher, M. Q., et al. (2018). Replacement times of a spectrum of elements in the North Atlantic based on thorium supply. *Global Biogeochemical Cycles*, *32*(9), 1294–1311. https://doi.org/10.1029/2017GB005839

Hayes, C. T., Anderson, R. F., Fleisher, M. Q., Serno, S., Winckler, G., & Gersonde, R. (2013). Quantifying lithogenic inputs to the North Pacific Ocean using the long-lived thorium isotopes. *Earth and Planetary Science Letters*, *383*, 16–25. https://doi.org/10.1016/j.epsl.2013.09.025

Hayes, C. T., Anderson, R. F., Fleisher, M. Q., Vivancos, S. M., Lam, P. J., Ohnemus, D. C., et al. (2015). Intensity of Th and Pa scavenging partitioned by particle chemistry in the North Atlantic Ocean. *Marine Chemistry*, *170*, 49–60. https://doi.org/10.1016/j.marchem.2015.01.006

Hayes, C. T., Fitzsimmons, J. N., Boyle, E. A., McGee, D., Anderson, R. F., Weisend, R., & Morton, P. L. (2015). Thorium isotopes tracing the iron cycle at the Hawaii Ocean Time-series Station ALOHA. *Geochimica et Cosmochimica Acta*, *169*, 1–16. https://doi.org/10.1016/j.gca.2015.07.019

Hayes, C. T., Rosen, J., McGee, D., & Boyle, E. A. (2017). Thorium distributions in high- and low-dust regions and the significance for iron supply. *Global Biogeochemical Cycles*, *31*(2), 328–347. https://doi.org/10.1002/2016GB005511

Hsieh, Y.-T., Henderson, G. M., & Thomas, A. L. (2011). Combining seawater ^{232}Th and ^{230}Th concentrations to determine dust fluxes to the surface ocean. *Earth and Planetary Science Letters*, *312*(3–4), 280–290. https://doi.org/10.1016/j.epsl.2011.10.022

Jickells, T., & Moore, C. M. (2015). The importance of atmospheric deposition for ocean productivity. *Annual Review of Ecology, Evolution, and Systematics*, *46*(1), 481–501. https://doi.org/10.1146/annurev-ecolsys-112414-054118

Lerner, P., Marchal, O., Lam, P. J., Buesseler, K., & Charette, M. (2017). Kinetics of thorium and particle cycling along the U.S. GEOTRACES North Atlantic Transect. *Deep Sea Research Part I: Oceanographic Research Papers*, *125*(April), 106–128. https://doi.org/10.1016/j.dsr.2017.05.003

Lopez, G. I., Marcantonio, F., Lyle, M., & Lynch-Stieglitz, J. (2015). Dissolved and particulate ^{230}Th–^{232}Th in the Central Equatorial Pacific Ocean: Evidence for far-field transport of the East Pacific Rise hydrothermal plume. *Earth and Planetary Science Letters*, *431*, 87–95. https://doi.org/10.1016/j.epsl.2015.09.019

Maher, B. A., Prospero, J. M., Mackie, D., Gaiero, D., Hesse, P. P., & Balkanski, Y. (2010). Global connections between aeolian dust, climate and ocean biogeochemistry at the present day and at the last glacial maximum. *Earth-Science Reviews*, *99*(1–2), 61–97. https://doi.org/10.1016/j.earscirev.2009.12.001

Martin, J. H. (1990). Glacial-interglacial CO_2 change: The iron hypothesis. *Paleoceanography*, *5*(1), 1–13. https://doi.org/10.1029/PA005i001p00001

Martínez-García, A., Sigman, D. M., Ren, H., Anderson, R. F., Straub, M., Hodell, D. A., et al. (2014). Iron fertilization of the Subantarctic Ocean during the last ice age. *Science*, *343*(6177), 1347–1350. https://doi.org/10.1126/science.1246848

McGee, D., Winckler, G., Borunda, A., Serno, S., Anderson, R. F., Recasens, C., et al. (2016). Tracking eolian dust with helium and thorium: Impacts of grain size and provenance. *Geochimica et Cosmochimica Acta*, *175*, 47–67. https://doi.org/10.1016/j.gca.2015.11.023

Measures, C. I., & Vink, S. (2000). On the use of dissolved aluminum in surface waters to estimate dust deposition to the ocean. *Global Biogeochemical Cycles*, *14*(1), 317–327. https://doi.org/10.1029/1999GB001188

Moran, S. B., Shen, C.-C., Edmonds, H. N. N., Weinstein, S. E. E., Smith, J. N. N., & Edwards, R. L. L. (2002). Dissolved and particulate ^{231}Pa and ^{230}Th in the Atlantic Ocean: Constraints on intermediate/deep water age, boundary scavenging, and ^{231}Pa/^{230}Th fractionation. *Earth and Planetary Science Letters*, *203*(3–4), 999–1014. https://doi.org/10.1016/S0012-821X(02)00928-7

Nozaki, Y., Horibe, Y., & Tsubota, H. (1981). The water column distributions of thorium isotopes in the western North Pacific. *Earth and Planetary Science Letters*, *54*(2), 203–216. https://doi.org/10.1016/0012-821x(81)90004-2

Owens, S. A., Buesseler, K. O., & Sims, K. W. W. (2011). Re-evaluating the 238U-salinity relationship in seawater: Implications for the 238U-234Th disequilibrium method. *Marine Chemistry*, *127*(1–4), 31–39. https://doi.org/10.1016/j.marchem.2011.07.005

Pavia, F. J., Anderson, R. F., Winckler, G., & Fleisher, M. Q. (2020). Atmospheric dust inputs, iron cycling, and biogeochemical connections in the South Pacific Ocean from thorium isotopes. *Global Biogeochemical Cycles*, *34*(9), 1–18. https://doi.org/10.1029/2020GB006562

Pérez-Tribouillier, H., Noble, T. L., Townsend, A. T., Bowie, A. R., & Chase, Z. (2020). Quantifying lithogenic inputs to the Southern Ocean using long-lived thorium isotopes. *Frontiers in Marine Science*, *7*, 207. https://doi.org/10.3389/fmars.2020.00207

Rowland, G. H., & Henderson, G. M. (2026). Dataset accompanying "An optimal approach for assessment of dust fluxes to the ocean using ^{232}Th and ^{230}Th" [Dataset]. *Zenodo*. https://doi.org/10.5281/ZENODO.18343942

Rowland, G. H., Hendry, K. R., Annett, A. L., Ng, H. C., Robinson, L. F., Sherrell, R. M., et al. (2025). High lithogenic and micro-nutrient fluxes from the West Greenland margin traced by thorium in seawater and sediments. *Global Biogeochemical Cycles*, *39*(10), e2025GB008531. https://doi.org/10.1029/2025GB008531

Rowland, G. H., Ng, H. C., Robinson, L. F., McManus, J. F., Mohamed, K. J., & McGee, D. (2017). Investigating the use of ^{232}Th/^{230}Th as a dust proxy using co-located seawater and sediment samples from the low-latitude North Atlantic. *Geochimica et Cosmochimica Acta*, *214*, 143–156. https://doi.org/10.1016/j.gca.2017.07.033

Roy-Barman, M., Chen, J. H. H., & Wasserburg, G. J. J. (1996). ^{230}Th–^{232}Th systematics in the central Pacific Ocean: The sources and the fates of thorium. *Earth and Planetary Science Letters*, *139*(3–4), 351–363. https://doi.org/10.1016/0012-821X(96)00017-9

Schlitzer, R. (2018). Ocean Data View (Version 5.8.2) [Software]. Retrieved from https://odv.awi.de

Schlitzer, R., Anderson, R. F., Dodas, E. M., Lohan, M., Geibert, W., Tagliabue, A., et al. (2018). The GEOTRACES Intermediate Data Product 2017. *Chemical Geology*, *493*, 210–223. https://doi.org/10.1016/J.CHEMGEO.2018.05.040

van der Does, M., Brummer, G. A., van Crimpen, F. C. J., Korte, L. F., Mahowald, N. M., Merkel, U., et al. (2020). Tropical rains controlling deposition of Saharan dust across the North Atlantic Ocean. *Geophysical Research Letters*, *47*(5), e2019GL086867. https://doi.org/10.1029/2019GL086867

Weis, J., Chase, Z., Schallenberg, C., Strutton, P. G., Bowie, A. R., & Fiddes, S. L. (2024). One-third of Southern Ocean productivity is supported by dust deposition. *Nature*, *629*(8012), 603–608. https://doi.org/10.1038/s41586-024-07366-4

Wu, C., Lin, Z., & Liu, X. (2020). The global dust cycle and uncertainty in CMIP5 (Coupled Model Intercomparison Project phase 5) models. *Atmospheric Chemistry and Physics*, *20*(17), 10401–10425. https://doi.org/10.5194/acp-20-10401-2020

Yu, H., Tan, Q., Chin, M., Remer, L. A., Kahn, R. A., Bian, H., et al. (2019). Estimates of African dust deposition along the trans-Atlantic transit using the decade long record of aerosol measurements from CALIOP, MODIS, MISR, and IASI. *Journal of Geophysical Research: Atmospheres*, *124*(14), 7975–7996. https://doi.org/10.1029/2019JD030574